THE EUROPEAN
PHYSICAL JOURNAL C

Regular Article - Theoretical Physics

The $\sin 2\phi_h$ azimuthal asymmetry of pion production in SIDIS within TMD factorization

Hui Li[1,2], **Zhun Lu**[1,a]

[1] School of Physics, Southeast University, Nanjing 211189, China
[2] School of Physics and Information Engineering, Shanxi Normal University, Taiyuan 030031, China

Abstract We study the $\sin 2\phi_h$ azimuthal asymmetry of charged and neutral pion productions off the longitudinally polarized nucleon targets in semi-inclusive deeply inelastic scattering (SIDIS) process within the transverse momentum dependent (TMD) factorization. The asymmetry is contributed by the convolution of the TMD distribution $h_{1L}^\perp$ and the Collins fragmentation function $H_1^\perp$. We adopt the Wandzura–Wilczek-type (WW-type) approximation for $h_{1L}^\perp$ and two different parametrizations on the nonperturbative Sudakov form factor for $h_{1L}^\perp$ and $H_1^\perp$. We estimate the $\sin 2\phi_h$ asymmetry at HERMES and CLAS and compare them with the corresponding experimental data. We also provide the prediction at kinematical configuration of CLAS12. It is shown that our theoretical calculation can describe the HERMES and CLAS data, except the asymmetry of the π^- production off proton target at HERMES and CLAS. We also find that different choices of the nonperturbative part of TMD evolution lead qualitatively similar results.

1 Introduction

Investigating the internal structure of the nucleon is still a frontier of hadronic physics. Of particular interests are the transverse momentum dependent distributions (TMDs) since it encode three-dimensional information of the nucleon in the momentum space structures [1–14], which is much richer than that of the collinear parton distribution functions. At leading twist, there are eight TMDs appearing in the decomposition of the quark-quark correlator of the nucleon [15–17]. Each of these TMDs, depending on the longitudinal momentum fraction x and the transverse momentum $\boldsymbol{p}_T$, represents a special spin and partonic structure of the nucleon. The essential tools to explore TMDs are the spin and azimuthal asymmetries in various polarized or unpolarized processes

involving at least two hadrons, such as SIDIS [18–29] and Drell–Yan [30–33] processes.

Among the leading-twist TMDs, the distribution $h_{1L}^\perp(x, \boldsymbol{p}_T^2)$ [34] is of particular interest. It describes the probability of finding a transversely polarized quark but inside a longitudinally polarized nucleon. Therefore, it is also called as the worm-gear distribution or longi-transversity. Since $h_{1L}^\perp$ is chiral odd, it has to be coupled to another chiral-odd function to manifest its effects in semi-inclusive processes. In SIDIS, this can be achieved via a $\sin 2\phi_\pi$ azimuthal asymmetry [34,35] when $h_{1L}^\perp$ is combined with the chiral-odd Collins function $H_1^\perp$ [36]. The early works on the $\sin 2\phi_\pi$ asymmetry in the longitudinally polarized SIDIS process have been performed in Refs. [37–44], showing that the asymmetry is around several percents.

In this paper, we perform a detailed phenomenological analysis of the $\sin 2\phi_h$ azimuthal asymmetry of the charged and neutral pion productions off the longitudinally polarized nucleon target in SIDIS within TMD factorization [45–49]. We estimate the $\sin 2\phi_h$ asymmetries and compare them with the corresponding experimental data at HERMES (deuteron and proton target) [37,38,50–52] and CLAS (proton target) [39,53]. We also provide the prediction at kinematical configuration of CLAS12 (proton target) [54]. We apply the TMD factorization to estimate the spin-dependent cross section in $l + N^\rightarrow \to l + \pi + X$ as well as the unpolarized cross section. The asymmetry can be expressed as the ratio of the two cross sections. In the last two decades, TMD factorization has become a powerful tool for studying the three-dimensional structure of the nucleon and has been widely applied in various high energy processes [45,47–49,55–67]. The TMD factorization theorem allows the differential cross section in the small transverse momentum region $P_T/z \ll Q$ (P_T is the transverse momentum of the detected particle and Q is the virtuality of the photon) to be expressed as a convolution of two contributions: one corresponds to the hard scattering factors at short distance; the other accounts for the

[a] e-mail: zhunlu@seu.edu.cn (corresponding author)

coherent long-distance interactions, and is described in terms of the well-defined TMDs. In our case, the $\sin 2\phi_h$ asymmetry is contributed by the convolution of longitudinal transversity PDF $h_{1L}^\perp$, Collins FF $H_1^\perp$ and the hard scattering factors. The TMD formalism also encodes the evolution information of TMDs, of which the energy evolution (or the scale dependence) are governed by the so-called Collins–Soper equation [45,46,49,68]. The solution of the equation is usually expressed as an exponential form of the Sudakov-like form factor [46,49,57,69] which indicates the change of TMDs from a initial scale to another scale. The Sudakov-like form factor can be separated to two parts. One is the perturbative part, which can be calculated perturbatively and is the same for different TMDs; the other is the nonperturbative part, which can not be calculated directly and is usually obtained by phenomenological extraction from experimental data. In the literature, several nonperturbative parts of the Sudakov form factor for the TMDs have been extracted from experimental data [46,49,57,60,62,64,70–80]. In this work, we will consider the TMD evolution effect of TMDs with two parameterizations on the nonperturbative part [62,64] to estimate the asymmetry for comparison.

The remaining content of the paper is organized as follows. In Sect. 2, we investigate the evolution effect for the TMDs. Particularly, we discuss the parametrization of the nonperturbative Sudakov form factors associated with the studied TMDs in details. In Sect. 3, we present the formalism of the $\sin 2\phi_h$ asymmetry in $lN^\rightarrow \to l\pi X$ within the TMD factorization. In Sect. 4, we numerically estimate the asymmetry $A_{UL}^{\sin 2\phi_h}$ in the $lN^\rightarrow \to l\pi X$ process at the kinematical region of HERMES, CLAS, CLAS12 with two different choices on the nonperturbative part associated with TMD evolution effect. Finally, We summarize the paper in Sect. 5.

2 The evolution of TMDs

In this section, we review the evolution formalism of the unpolarized TMD f_1, the distribution $h_{1L}^\perp$ of the nucleon as well as the unpolarized fragmentation function D_1, the Collins function $H_1^\perp$ of the pion, within the TMD factorization.

Usually, the TMD evolution is performed in coordinate b-space, as in this case the cross section can be expressed as a product of TMDs in b-space [46,49]. In the TMD factorization based on different schemes (such as the CS-81 [45], JMY [47,48] and Collins-11 schemes [49]), the TMDs $\tilde{F}(x, b; \mu, \zeta_F)$ and $\tilde{D}(z, b; \mu, \zeta_D)$) depend on two energy scales [45,46,49,57,59,74]. One is the renormalization scale μ, the other is the energy scale ζ_F (or ζ_D) serving as a cutoff to regularize the light-cone singularity in the operator definition of the TMDs. As is well known, the Collins–Soper (CS)

equation [45] (in this paper $b = |\boldsymbol{b}_\perp|$ and the tilde terms represent the ones in b space) determines the ζ_F (or ζ_D) dependence of the TMD PDFs (or FFs):

$$\frac{\partial \ln \tilde{F}(x, b; \mu, \zeta_F)}{\partial \sqrt{\zeta_F}} = \frac{\partial \ln \tilde{D}(z, b; \mu, \zeta_D)}{\partial \sqrt{\zeta_D}} = \tilde{K}(b; \mu), \quad (1)$$

with $\tilde{K}$ being the CS evolution kernel which can be computed perturbatively for small values of b(up to order α_s):

$$\tilde{K}(b; \mu) = -\frac{\alpha_s C_F}{\pi} \left[\ln(\mu^2 b^2) - \ln 4 + 2\gamma_E \right] + \mathcal{O}(\alpha_s^2), \tag{2}$$

and $\gamma_E \approx 0.577$ is the Euler's constant [45].

On the other hand, the μ dependence of the TMDs is derived from the renormalization group equation

$$\frac{d \tilde{K}}{d \ln \mu} = -\gamma_K(\alpha_s(\mu)), \tag{3}$$

$$\frac{d \ln \tilde{F}(x, b; \mu, \zeta_F)}{d \ln \mu} = \gamma_F(\alpha_s(\mu); \frac{\zeta_F^2}{\mu^2}), \tag{4}$$

$$\frac{d \ln \tilde{D}(z, b; \mu, \zeta_D)}{d \ln \mu} = \gamma_D(\alpha_s(\mu); \frac{\zeta_D^2}{\mu^2}), \tag{5}$$

where γ_K, γ_F and γ_D are the anomalous dimensions of $\tilde{K}$, $\tilde{F}$ and $\tilde{D}$, respectively,

$$\gamma_K = 2\frac{\alpha_s C_F}{\pi} + \mathcal{O}(\alpha_s^2), \tag{6}$$

$$\gamma_D = \gamma_F = \alpha_s \frac{C_F}{\pi} \left(\frac{3}{2} - \ln \left(\frac{\zeta_F}{\mu^2} \right) \right) + \mathcal{O}(\alpha_s^2). \tag{7}$$

Solving Eqs. (1) and (3-5), one can obtain the general solution for the energy dependence of $\tilde{F}$ (or $\tilde{D}$) [45–49,68, 78]:

$$\tilde{F}(x, b; Q) = \mathcal{F} \times e^{-S(Q,b)} \times \tilde{F}(x, b; \mu_i), \tag{8}$$

$$\tilde{D}(z, b; Q) = \mathcal{D} \times e^{-S(Q,b)} \times \tilde{D}(z, b; \mu_i). \tag{9}$$

Here, $\mathcal{F}$ and $\mathcal{D}$ are the factors related to the hard scattering, $S(Q, b)$ is the Sudakov form factor. Hereafter, we set $\mu = \sqrt{\zeta_F} = \sqrt{\zeta_D} = Q$, and express $\tilde{F}(x, b; \mu = Q, \zeta_F = Q^2)$ (or $\tilde{D}(z, b; \mu = Q, \zeta_D = Q^2)$) as $\tilde{F}(x, b; Q)$ (or $\tilde{D}(z, b; Q)$) for simplicity. Eq. (8) (or Eq. (9)) demonstrates that the distribution $\tilde{F}$ (or $\tilde{D}$) at an arbitrary scale Q can be determined by the same distribution at an initial scale μ_i through the evolution encoded by the exponential form $\exp(-S(Q, b))$.

Specifically, the exponential $\exp(-S(Q,b))$ for $\tilde{F}$ has the following explicit form (similar form holds for $\tilde{D}$)

$$
\exp(-S(Q,b)) = \exp\left\{ \ln\frac{Q}{\mu}\tilde{K}(b_*;\mu) + \int_{\mu_i}^{\mu}\frac{d\bar{\mu}}{\bar{\mu}} \right.
$$
$$
\left. \times\left[\gamma_F(g(\bar{\mu});1) - \ln\left(\frac{Q}{\bar{\mu}}\right)\gamma_K(g(\bar{\mu})) \right] \right\}
$$
$$
\times \exp\left\{ g_{j/P}(x,b) + g_K(b)\ln\frac{Q}{Q_0} \right\}. \tag{10}
$$

The exponential in the first line of Eq. (10) comes from the solutions of Eqs. (1), (3) and (4) in the perturbative region (the small b region $b \ll 1/\Lambda$). It contains $\tilde{K}(b_*;\mu)$, the CS evolution kernel in the small b region; and the anomalous dimension γ_F, γ_K. However, in the nonperturbative region (large b region), the evolution kernel $\tilde{K}(b;\mu)$ is not calculable. In order to obtain the information in the large b region, the exponential in the second line of Eq. (10) is introduced. The function $g_{j/P}(x,b)$ parameterizes the non-perturbative large-b behavior which is intrinsic to the proton target, while the universal function g_K parameterizes the non-perturbative large-b behavior of the evolution kernel $\tilde{K}(b;\mu)$.

To allow a smooth transition of b from perturbative region to nonperturbative region as well as to avoid hitting on the Landau pole, one can set a parameter $b_{\max}$ to be the boundary between the two regions. The typical value of $b_{\max}$ is chosen around 1 GeV^{-1} to guarantee that b_* is always in the perturbative region. A b-dependent function $b_*(b)$ may be also introduced to have the property $b_* \approx b$ at small b value and $b_* \approx b_{\max}$ at large b value. There are several different choices on the expression of $b_*(b)$ in the literature [46,64,81]. A frequently used one is the Collins–Soper–Sterman (CSS) prescription [46]:

$$
b_* = b/\sqrt{1 + b^2/b_{\max}^2}, \ \ b_{\max} < 1/\Lambda_{\text{QCD}}. \tag{11}
$$

Combining the perturbative part and the nonperturbative part, one has the complete result for the Sudakov form factor appearing in Eqs. (8) and (9):

$$
S(Q,b) = S_{\text{P}}(Q,b_*) + S_{\text{NP}}(Q,b), \tag{12}
$$

with the boundary of the two parts set by the $b_{\max}$. The perturbative part $S_{\text{P}}(Q,b_*)$ has been studied [59,62,74,75,77] in details and has the following form:

$$
S_{\text{P}}(Q,b_*) = \int_{\mu_b^2}^{Q^2}\frac{d\bar{\mu}^2}{\bar{\mu}^2}\left[A(\alpha_s(\bar{\mu}))\ln\frac{Q^2}{\bar{\mu}^2} + B(\alpha_s(\bar{\mu})) \right], \tag{13}
$$

which is the same for different kinds of PDFs and FFs, namely, S_P is spin-independent. The coefficients A and B in Eq. (13) can be expanded as the series of α_s/π:

$$
A = \sum_{n=1}^{\infty} A^{(n)}\left(\frac{\alpha_s}{\pi}\right)^n, \tag{14}
$$

$$
B = \sum_{n=1}^{\infty} B^{(n)}\left(\frac{\alpha_s}{\pi}\right)^n. \tag{15}
$$

In this work, we will take $A^{(n)}$ up to $A^{(2)}$ and $B^{(n)}$ up to $B^{(1)}$ in the accuracy of next-to-leading-logarithmic (NLL) order [46,57,59,72,75,82]:

$$
A^{(1)} = C_F, \tag{16}
$$

$$
A^{(2)} = \frac{C_F}{2}\left[C_A\left(\frac{67}{18} - \frac{\pi^2}{6}\right) - \frac{10}{9}T_R n_f \right], \tag{17}
$$

$$
B^{(1)} = -\frac{3}{2}C_F, \tag{18}
$$

with $C_F = 4/3$, $C_A = 3$ and $T_R = 1/2$.

The non-perturbative part S_{NP} in Eq. (12) can not be calculated perturbatively, it is usually parameterized and extracted from experimental data. There are several extractions for S_{NP} by different groups literature [46,49,57,60,62,64,70–80], we will discuss two of them in details to investigate the impact of the different evolution formalisms on the asymmetry.

One of the parameterizations applied in this study is the Echevarria–Idilbi–Kang–Vitev (EIKV parametrization) non-perturbative Sudakov S_{NP} for the unpolarized TMD PDFs (or TMD FFs), which has the following form [62]:

$$
S_{\text{NP}}^{\text{pdf}}(b,Q) = b^2\left(g_1^{\text{pdf}} + \frac{g_2}{2}\ln\frac{Q}{Q_0} \right), \tag{19}
$$

$$
S_{\text{NP}}^{\text{ff}}(b,Q) = b^2\left(g_1^{\text{ff}} + \frac{g_2}{2}\ln\frac{Q}{Q_0} \right). \tag{20}
$$

Here, g_2 includes the information on the large b behavior of the evolution kernel $\tilde{K}$ ($g_K(b) = g_2 b^2$). This function is universal for different types of TMDs and does not depend on the particular process, which is an important prediction of QCD factorization theorems involving TMDs [49,57,62,63]. g_1 contains information on the intrinsic nonperturbative transverse motion of bound partons. It could depend on the type of TMDs, and can be interpreted as the intrinsic transverse momentum width for the relevant TMDs at the initial scale Q_0 [57,76,82–84]. Furthermore, g_1^{pdf} and g_1^{ff} are parameterized as:

$$
g_1^{\text{pdf}} = \frac{\langle k_T^2 \rangle_{Q_0}}{4}, \tag{21}
$$

$$
g_1^{\text{ff}} = \frac{\langle p_T^2 \rangle_{Q_0}}{4z^2}, \tag{22}
$$

where $\langle k_T^2 \rangle_{Q_0}$ and $\langle p_T^2 \rangle_{Q_0}$ are the averaged intrinsic transverse momenta squared for TMD PDFs and FFs at the initial

scale Q_0, respectively. In Ref. [62] the authors tuned the current extracted ranges of three parameters $\langle k_T^2 \rangle_{Q_0}$, $\langle p_T^2 \rangle_{Q_0}$ and g_2 with $Q_0 = \sqrt{2.4}$ GeV in Refs. [85–87] and further found that the following fixed values of parameters can reasonably describe the SIDIS data together with the Drell–Yan lepton pair and W/Z boson production data:

$$\langle k_T^2 \rangle_{Q_0} = 0.38 \, \text{GeV}^2, \qquad \langle p_T^2 \rangle_{Q_0} = 0.19 \, \text{GeV}^2,$$
$$g_2 = 0.16 \, \text{GeV}^2, \quad b_{\max} = 1.5 \, \text{GeV}^{-1}. \tag{23}$$

Besides the Sudakov form factor in Eqs. (8) and (9), another important element in Eqs. (8) and (9) is the TMDs at a fixed scale μ. In the small b region, $\tilde{F}(x, b; \mu)$ and $\tilde{D}(x, b; \mu)$ at a fixed scale μ can be expressed as the convolution of the perturbatively calculable coefficients C and the corresponding collinear counterparts $F_{i/H}(\xi, \mu)$ (or $D_{H/j}(\xi, \mu)$),

$$\tilde{F}(x, b; \mu) = \sum_i \int_x^1 \frac{d\xi}{\xi} C_{q \leftarrow i}(x/\xi, b; \mu) F_{i/H}(\xi, \mu), \tag{24}$$

$$\tilde{D}(z, b; \mu) = \sum_j \int_z^1 \frac{d\xi}{\xi} C_{j \leftarrow q}(z/\xi, b; \mu) D_{H/j}(\xi, \mu), \tag{25}$$

Here, μ is a dynamic scale related to b_* by $\mu = c/b_*$, with $c = 2e^{-\gamma_E}$ and $\gamma_E \approx 0.577$ being the Euler's constant [45], $C_{q \leftarrow i}(x/\xi, b; \mu) = \sum_{n=0}^{\infty} C_{q \leftarrow i}^{(n)}(\alpha_s/\pi)^n$ and $C_{j \leftarrow q}(z/\xi, b; \mu) = \sum_{n=0}^{\infty} C_{j \leftarrow q}^{(n)}(\alpha_s/\pi)^n$ are the perturbatively calculable coefficient function.

After solving the evolution equations and incorporating the Sudakov form factor, the scale-dependent TMDs in b space can be rewritten as

$$\tilde{F}_{q/H}(x, b; Q) = e^{-\frac{1}{2}S_P(Q, b_*) - S_{NP}^{F_{q/H}}(Q, b)} F_{q/H}(x, \mu), \tag{26}$$

$$\tilde{D}_{H/q}(z, b; Q) = e^{-\frac{1}{2}S_P(Q, b_*) - S_{NP}^{D_{H/q}}(Q, b)} D_{H/q}(z, \mu). \tag{27}$$

The factor of $\frac{1}{2}$ in front of S_P comes from the fact that S_P is equally distributed to the initial-state quark and the final-state quark [88]. The hard coefficients C, $\mathcal{F}$ and $\mathcal{D}$ for f_1, D_1 and $H_1^\perp$ have been calculated up to next-to-leading order (NLO), and those for the $h_{1L}^\perp$ are also known up to NLO [89]. However, only the first term of the $h_{1L}^\perp$ result in Eq. (57) of Ref. [89], namely the $\tilde{h}(x)$ term, is dominant. It is not necessary to consider the $\tilde{T}_F^{(\sigma)}$ contribution in this paper as it is beyond the WW-approximation and a very extensive project. For consistency, in this work we adopt the LO results for the hard coefficients C, $\mathcal{F}$ and $\mathcal{D}$ for f_1, $h_{1L}^\perp$, D_1 and $H_1^\perp$, i.e. $C_{q \leftarrow i}^{(0)} = \delta_{iq}\delta(1-x)$, $C_{j \leftarrow q}^{(0)} = \delta_{qj}\delta(1-z)$, $\mathcal{F} = 1$ and $\mathcal{D} = 1$.

With all the ingredients above, we can obtain the unpolarized TMD of the nucleon $\tilde{f}_1^{q/p}$ (or the unpolarized fragmentation of the pion $\tilde{D}_1^{\pi/q}$) in b space

$$\tilde{f}_1^{q/p}(x, b; Q) = e^{-\frac{1}{2}S_P(Q, b_*) - S_{NP}^{pdf}(Q, b)} f_1^{q/p}(x, \mu), \tag{28}$$

$$\tilde{D}_1^{\pi/q}(z, b; Q) = e^{-\frac{1}{2}S_P(Q, b_*) - S_{NP}^{ff}(Q, b)} D_1^{\pi/q}(z, \mu). \tag{29}$$

By performing the Fourier transformation, we can obtain the TMDs in the transverse momentum space

$$f_1^{q/N}(x, \boldsymbol{p}_T; Q)$$
$$= \int_0^\infty \frac{dbb}{2\pi} J_0(|\boldsymbol{p}_T|b) e^{-\frac{1}{2}S_P(Q, b_*) - S_{NP}^{pdf}(Q, b)} f_1^{q/p}(x, \mu), \tag{30}$$

$$D_1^{\pi/q}(z, \boldsymbol{K}_\perp; Q)$$
$$= \int_0^\infty \frac{dbb}{2\pi} J_0(|\boldsymbol{K}_\perp|b/z) e^{-\frac{1}{2}S_P(Q, b_*) - S_{NP}^{ff}(Q, b)}$$
$$\times D_1^{\pi/q}(z, \mu). \tag{31}$$

According to Eqs. (24) and (25), in the small b region, we can also express the longitudinal transversity PDF of nucleon target $\tilde{h}_{1L}^\perp$ and the Collins FF of pion production $\tilde{H}_1^\perp$ at a fixed energy scale μ in terms of the perturbatively calculable coefficients and the corresponding collinear correlation function [63,90]:

$$\tilde{h}_{1L}^{\perp(\beta)q/N}(x, b; \mu) = ib^\beta M_N h_{1L}^{\perp(1)}(x, \mu), \tag{32}$$

$$\tilde{H}_1^{\perp(\alpha)\pi/q}(z, b; \mu) = -\frac{ib^\alpha}{2z} \hat{H}^{(3)}(z, z, \mu), \tag{33}$$

where the superscript (1) denotes the first transverse moment of the function:

$$h_{1L}^{\perp(1)}(x) = \int d^2p_T \frac{p_T^2}{2M^2} h_{1L}^\perp(x,) \tag{34}$$

The hard coefficients in Eqs. (36) and (37) are calculated up to LO, and $\hat{H}^{(3)}(z, z, \mu)$ is defined in Ref. [63], which differs by a factor of $(-1/z)$ from Ref. [90]. Furthermore, the longitransversity of the nucleon target and the Collins FF of the pion in the b-space are defined as

$$\tilde{h}_{1L}^{\perp\beta, q/N}(x, b; \mu)$$
$$= \int d^2\boldsymbol{p}_T e^{-i\boldsymbol{p}_T \cdot b} \frac{p_T^\beta}{M_N} h_{1L}^{\perp q/N}(x, \boldsymbol{p}_T^2; \mu),$$
$$\tilde{H}_1^{\perp\alpha, \pi/q}(z, b; \mu)$$
$$= \int d^2\boldsymbol{K}_\perp e^{-i\boldsymbol{K}_\perp \cdot b/z} \frac{\boldsymbol{K}_\perp^\alpha}{M_\pi} H_1^{\perp\pi/q}(z, \boldsymbol{K}_\perp^2; \mu). \tag{35}$$

As for the nonperturbative part of the Sudakov form factor associated with the longi-transversity and the Collins function, the information still remains unknown. In a practical calculation, we assume that they are respectively the same as S_{NP}^{pdf} and S_{NP}^{ff}. Therefore, we can obtain the the longi-transversity and the Collins function in b-space as

$$
\begin{aligned}
&\tilde{h}_{1L}^{\perp(\beta)q/N}(x, b; Q) \\
&= ib^\beta M_N e^{-\frac{1}{2}S_P(Q,b_*)-S_{NP}^{pdf}(Q,b)} \tilde{h}_{1L}^{\perp(1)}(x, \mu),
\end{aligned}
\tag{36}
$$

$$
\begin{aligned}
&\tilde{H}_1^{\perp(\alpha)\pi/q}(z, b; Q) \\
&= -\frac{ib^\alpha}{2z} e^{-\frac{1}{2}S_P(Q,b_*)-S_{NP}^{ff}(Q,b)} \hat{H}^{(3)}(z, z, \mu).
\end{aligned}
\tag{37}
$$

After performing the Fourier transformation, one can obtain the TMDs in the transverse momentum space

$$
\begin{aligned}
&\frac{p_\perp^\beta}{M_N} \tilde{h}_{1L}^{\perp q/N(\beta)}(x, p_T; Q) \\
&= M_N \int_0^\infty \frac{db\, b^2}{2\pi} J_1(|\boldsymbol{p}_T|b) e^{-\frac{1}{2}S_P(Q,b_*)-S_{NP}^{pdf}(Q,b)} \\
&\quad \times \tilde{h}_{1L}^{\perp(1)}(x, \mu),
\end{aligned}
\tag{38}
$$

$$
\begin{aligned}
&\frac{K_\perp^\alpha}{M_\pi} \tilde{H}_1^{\perp\pi/q(\alpha)}(z, K_\perp; Q) \\
&= -\frac{1}{z} \int_0^\infty \frac{db\, b^2}{4\pi} J_1(|\boldsymbol{K}_\perp|b/z) e^{-\frac{1}{2}S_P(Q,b_*)-S_{NP}^{ff}(Q,b)} \\
&\quad \times \hat{H}^{(3)}(z, z, \mu).
\end{aligned}
\tag{39}
$$

Besides the EIKV parametrization on non-perturbative factor S_{NP} mentioned above, another parametrization applied in this study is the Bacchetta, Delcarro, Pisano, Radici and Signori (BDPRS) parameterization S_{NP} for the unpolarized TMDs, which has the following form [64]:

$$
\begin{aligned}
&\tilde{f}_1^a(x, b; Q) \\
&= f_1^a(x; \mu^2) e^{-S(\mu,Q)} e^{\frac{1}{2}g_K(b)\ln(Q^2/Q_0^2)} \tilde{f}_{1NP}^a(x, b),
\end{aligned}
\tag{40}
$$

$$
\begin{aligned}
&\tilde{D}_1^{a\to h}(z, b; Q) \\
&= D_1^{a\to h}(z; \mu^2) e^{-S(\mu,Q)} e^{\frac{1}{2}g_K(b)\ln(Q^2/Q_0^2)} \tilde{D}_{1NP}^{a\to h}(z, b),
\end{aligned}
\tag{41}
$$

where $g_K = -g_2 b^2/2$, following the choice in Refs. [72,73,79]. $\tilde{f}_{1NP}^a(x, b^2)$ and $\tilde{D}_{1NP}^{a\to h}(z, b^2)$ are the intrinsic nonperturbative part of the PDFs and FFs respectively, which are parameterized as

$$
\tilde{f}_{1NP}^a(x, b^2) = \frac{1}{2\pi} e^{-g_1\frac{b^2}{4}} \left(1 - \frac{\lambda g_1^2}{1+\lambda g_1}\frac{b^2}{4}\right),
\tag{42}
$$

$$
\tilde{D}_{1NP}^{a\to h}(z, b^2) = \frac{g_3 e^{-g_3\frac{b^2}{4z^2}} + \left(\frac{\lambda_F}{z^2}\right) g_4^2 \left(1 - g_4\frac{b^2}{4z^2}\right) e^{-g_4\frac{b^2}{4z^2}}}{2\pi z^2 \left(g_3 + \left(\frac{\lambda_F}{z^2}\right) g_4^2\right)},
\tag{43}
$$

with

$$
g_1(x) = N_1 \frac{(1-x)^\alpha x^\sigma}{(1-\hat{x})^\alpha \hat{x}^\sigma},
\tag{44}
$$

$$
g_{3,4}(z) = N_{3,4} \frac{(z^\beta + \delta)(1-z)^\gamma}{(\hat{z}^\beta + \delta)(1-\hat{z})^\gamma}.
\tag{45}
$$

Here, $\hat{x} = 0.1$ and $\hat{z} = 0.5$ are fixed, and $\alpha, \sigma, \beta, \gamma, \delta$, $N_1 \equiv g_1(\hat{x})$, $N_{3,4} \equiv g_{3,4}(\hat{z})$ are free parameters fitted to the available data from SIDIS, Drell–Yan, and W/Z boson production processes. Besides the $b_*(b)$ prescription in the original CSS approach [46], there are also several different choices on the form of $b_*(b)$ [64,81]. In Ref. [64], a new b_* prescription different from Eq. (11) was proposed as

$$
b_* = b_{max} \left(\frac{1 - e^{-b^4/b_{max}^4}}{1 - e^{-b^4/b_{min}^4}}\right)^{1/4}
\tag{46}
$$

Again, b_{max} is the boundary of the nonperturbative and perturbative b space region with fixed value of $b_{max} = 2e^{-\gamma_E}$ GeV$^{-1} \approx 1.123$ GeV^{-1}. Furthermore, the authors in Ref. [64] also chose to saturate b_* at the minimum value $b_{min} \propto 2e^{-\gamma_E}/Q$.

3 The formalism of $\sin 2\phi_h$ asymmetry of pion production in SIDIS

In this section we will set up the necessary framework for physical observables in SIDIS process within TMD factorization by considering the evolution effects of TMDs. The process under study is:

$$
l(\ell) + N^{\to}(P) \to l(\ell') + \pi(P_\pi) + X,
\tag{47}
$$

the lepton beam with momentum ℓ scatters off a longitudinally polarized nucleon target N with momentum P. In the final state, the scattered lepton momentum ℓ' is measured together with an unpolarized final state hadron h (in this work h is the π meson). We define the space-like momentum transfer $q = \ell - \ell'$ and introduce the relevant kinematic invariants

$$
x = \frac{Q^2}{2P \cdot q}, \quad y = \frac{P \cdot q}{P \cdot \ell} = \frac{Q^2}{x_B s}, \quad z = \frac{P \cdot P_\pi}{P \cdot q},
$$
$$
Q^2 = -q^2, \quad s = (P + \ell)^2.
\tag{48}
$$

Here, s is the total center of mass energy squared, x is the Bjorken variable, y is the inelasticity and z is the momentum fraction of the final state hadron.
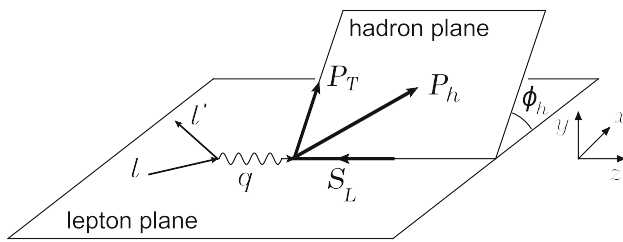
Fig. 1 The kinematical configuration for the SIDIS process. The initial and scattered leptonic momenta define the lepton plane ($x - z$ plane), while the detected hadron momentum together with the z axis identify the hadron production plane, the longitudinal spin of the nucleon is along the $-z$ axis

To leading order in $1/Q$ the SIDIS cross-section (for a longitudinally polarized nucleon target) is given by [17]

$$\frac{d^5\sigma}{dx\,dy\,dz\,d\phi_h\,dP_{\pi T}^2} = \frac{2\pi\alpha^2}{x_B y Q^2} \times \left\{ \left(1 - y + \frac{1}{2}y^2\right) F_{UU} \right.$$
$$\left. + (1-y)S_L \sin 2\phi_h F_{UL}^{\sin 2\phi_h} \right\}. \quad (49)$$

The corresponding reference frame of the process is given in Fig. 1. In this frame, the virtual photon momentum q defines the z-axis, the hadron plane is determined by the z-axis and the momentum direction of the final-state hadron, and the lepton plane is determined by the momentum direction of ℓ and ℓ'. Hence ϕ_h is the azimuthal angle of the final-state hadron with respect to the lepton plane; $P_{\pi T}$ is the component of P_π transverse with respect to q with $P_{\pi T} = -z q_T$ [91]. TMD factorization has been shown to be valid for SIDIS process only with $P_{\pi T}^2/z^2 \ll Q^2$ [49]. F_{UU} and $F_{UL}^{\sin 2\phi_h}$ are the spin-averaged and spin-dependent structure functions.

The expression for the $\sin 2\phi_h$ azimuthal asymmetry is given by

$$A_{UL}^{\sin 2\phi_h}(x, y, z, P_{\pi T}) = \frac{\frac{1}{xyQ^2}(1-y)F_{UL}^{\sin 2\phi_h}}{\frac{1}{xyQ^2}\left(1 - y + \frac{1}{2}y^2\right)F_{UU}}. \quad (50)$$

According to TMD factorization, the structure functions F_{UU} and $F_{UL}^{\sin 2\phi_\pi}$ are given in terms of an integral which convolutes transverse parton momentum in the distribution and the fragmentation function [34,35]

$$F_{UU}(x, z, Q; P_{\pi T}^2)$$
$$= x \sum_q e_q^2 \int d^2 p_T d^2 k_T \delta^2(p_T - k_T + q_T)$$
$$\times f_1^{q/N}(x, p_T^2; Q) D_1^{\pi/q}(z, k_T^2; Q), \quad (51)$$
$$F_{UL}^{\sin 2\phi_h}(x, z, Q; P_{\pi T})$$
$$= x \sum_q e_q^2 \int d^2 p_T d^2 k_T \delta^2(p_T - k_T + q_T)$$

$$\times \left[-\frac{2(\hat{h} \cdot k_T)(\hat{h} \cdot p_T) - k_T \cdot p_T}{M_N M_\pi} \right]$$
$$\times h_{1L}^{\perp q/N}(x, p_T^2; Q) H_1^{\perp \pi/q}(z, k_T^2; Q), \quad (52)$$

where the unit vector $\hat{h}$ is defined as $\hat{h} = P_{\pi T}/P_{\pi T}$, and the transverse momentum k_T is related to the transverse momentum of the produced hadron with respect to the quark through $K_\perp = -z k_T$.

For simplicity, we perform the TMD evolution effect in the b space which express the cross section with simple products of b-dependent TMDs in contrast to the complicated convolutions in the transverse momentum space. Performing a transformation for the delta function, we obtain the following explicit form of the spin-averaged structure function F_{UU}

$$F_{UU}(x, z, Q; P_{\pi T})$$
$$= x \frac{1}{z^2} \sum_q e_q^2 \int \frac{d^2 b}{(2\pi)^2} e^{i P_{\pi T} \cdot b/z} \tilde{f}_1^{q/N}(x, b; Q)$$
$$\times \tilde{D}_1^{\pi/q}(z, b; Q)$$
$$= x \frac{1}{z^2} \sum_q e_q^2 \int \frac{dbb}{2\pi} J_0(|P_{\pi T}||b|/z) \tilde{f}_1^{q/N}(x, b; Q)$$
$$\times \tilde{D}_1^{\pi/q}(z, b; Q)$$
$$= x \frac{1}{z^2} \sum_q e_q^2 \int \frac{dbb}{2\pi} J_0(|P_{\pi T}||b|/z) f_1^{q/N}(x, \mu)$$
$$\times D_1^{\pi/q}(z, \mu) e^{-(S_P(Q,b_*)+S_{NP}^{pdf}(Q,b)+S_{NP}^{ff}(Q,b))}. \quad (53)$$

Similarly, the spin-dependent structure function $F_{UL}^{\sin(2\phi_h)}$ can be written as

$$F_{UL}^{\sin 2\phi_h}(x, z, Q; P_{\pi T})$$
$$= x \frac{1}{z^3} \sum_q e_q^2 \int d^2 p_T d^2 K_\perp \int \frac{d^2 b}{(2\pi)^2}$$
$$\times e^{-i(p_T + K_\perp/z - P_{\pi T}/z) \cdot b}$$
$$\times [2(\hat{h} \cdot K_\perp)(\hat{h} \cdot p_T) - K_\perp \cdot p_T]$$
$$\times \frac{h_{1L}^{\perp q/N}(x, p_T^2; Q) H_1^{\perp \pi/q}(z, K_\perp^2; Q)}{M_N M_\pi}$$
$$= x \frac{1}{z^3} \sum_q e_q^2 \int \frac{d^2 b}{(2\pi)^2} e^{i P_{\pi T} \cdot b/z} (2\hat{h}_\alpha \hat{h}_\beta - g_{\alpha\beta}) \tilde{h}_{1L}^{\perp \beta, q/N}$$
$$\times (x, b; Q) \tilde{H}_1^{\perp \alpha, \pi/q}(z, b; Q)$$
$$= -x \frac{1}{z^4} \sum_q e_q^2 \int \frac{dbb^3}{4\pi} J_2(|P_{\pi T}||b|/z)$$
$$\times M_N h_{1L}^{\perp(1), q/N}(x; \mu) \hat{H}^{(3),\pi/q}(z, z; \mu)$$
$$\times e^{-(S_P(Q,b_*)+S_{NP}^{pdf}(Q,b)+S_{NP}^{ff}(Q,b))}. \quad (54)$$

Therefore, we obtain the evolved form of the structure functions $F_{UU}(x, z, Q; P_{\pi T})$ and $F_{UL}^{\sin 2\phi_h}(x, z, Q; P_{\pi T})$.

4 Numerical calculation

In this section, using the framework set up above, we present the numerical calculation of the $\sin 2\phi_h$ azimuthal asymmetry for π production in the process $lN^{\rightarrow} \rightarrow l\pi X$ off the longitudinally polarized nucleon. We estimate the asymmetry at the kinematical configurations of HERMES, CLAS and CLAS12, and compare it with the recent experimental measurements [37–39,52–54,92–95]. For this purpose we need to know the collinear functions appearing in Eqs. (53) and (54) as the inputs of the evolution. For the unpolarized PDF $f_1(x, \mu)$ of the nucleon, we apply the NLO set of the CT10 parametrization (central PDF set) [96]. For the unpolarized FF $D_1(z, \mu)$ of the pion, we apply the NLO set of the de Florian, Sassot, Stratmann (DSS) FF [97]. For the twist-3 Collins FF $H^{(3)}(z, z, \mu)$ of the pion, we adopt the parametrization given in Ref. [63].

Since $h_{1L}^{\perp}$ has not been extracted from experimental data, we obtain $h_{1L}^{\perp(1)}(x, \mu)$ by employing the WW-type approximation [98,99]. This approximation originates from the assumption [98] that the quark-quark-gluon correlation (or the pure twist-3 part) and the current-quark mass term in the decomposition of the operator definition of certain distributions can be ignored. It is found that the WW-approximation works well in interpreting the data of the twist-3 structure function $g_2(x)$ (or the distribution $g_T(x)$) in DIS [51,100–106]. It was also supported by lattice QCD calculation [107,108] and theoretical study from the instanton model [109,110]. In the WW-type approximation one can obtain the $h_L(x)$ as follows [99]

$$
h_L(x) = 2x \int_x^1 \frac{dy}{y^2} h_1(y) + \tilde{h}_L(x)^{WW-type}
$$
$$
\approx 2x \int_x^1 \frac{dy}{y^2} h_1^a(y), \tag{55}
$$

which contain twist-2 part $h_1(y)$ and pure twist-3 part $\tilde{h}_L(x)$ coming from the quark-quark-gluon correlation, and the later one may is neglected, within the WW-approximation. At the same time, we should also note that the WW-approximation has limitations in some cases. As pointed in Ref. [111], the pure twist-3 terms will break the WW-relation for the structure function g_2 (or $g_T(x)$) as large as 15%-40% the size of g_2. This means that in the case of $h_{1L}^{\perp}$ the higher-twist contribution may be also non-negligible and bring uncertainties to the results of the $\sin 2\phi_h$ asymmetry.

In addition, one also obtain the following relation in a similar way

$$
xh_L(x, p_T^2) \overset{WW-type}{\approx} -\frac{p_T^2}{M^2} h_{1L}^{\perp}(x, p_T^2). \tag{56}
$$

Thus, $h_{1L}^{\perp(1)}(x)$ is connected to the transversity distribution via the relation [106]

$$
h_{1L}^{\perp(1)}(x) \overset{WW-type}{\approx} -x^2 \int_x^1 \frac{dy}{y^2} h_1(y). \tag{57}
$$

In this work, we use the extractions of $h_1(y)$ from Ref. [63].

As for the energy evolution for $h_{1L}^{\perp(1)}$, it has been studied extensively in Ref. [112] and has a rather complicated form. Namely, the evolution kernel contains the homogeneous part and the inhomogeneous part. For the former one, it corresponds to the diagonal part of the operator for the distribution, while the latter one involves the nondiagonal part. As there is no any theoretical calculation and phenomenological extraction on the nondiagonal part of the operator for $h_{1L}^{\perp(1)}$, in this work following the choice in Refs. [63,66] to keep the diagonal part in the phenomenological calculations for the TMD evolutions. This is of course an approximation to the real situation and will bring further uncertainty coming from the nondiagonal part to the result of the asymmetry. In the literature only the nondiagonal part for the Qui-Sterman function $T_{q,F}$ has been studied [113] by using a model, which shows that nondiagonal terms in the evolution equation for $T_{q,F}(x, x)$ play a significant role in modifying the evolution of these correlation functions in the small x region. We expect similar pattern may hold for the evolution of $h_{1L}^{\perp(1)}$. For the question how large the uncertainty from the nondiagonal part should be, we will leave it as a future study.

Thus in this work we follow the similar option to consider the homogeneous terms of the $h_{1L}^{\perp(1)}$ evolution kernel:

$$
P_{qq}^h = C_F \left[\frac{2x}{(1-x)_+} + 2\delta(1-x) \right] - \frac{C_A}{2} \frac{2x}{1-x}. \tag{58}
$$

As for the evolution kernel of the twist-3 fragmentation function $\hat{H}^{(3)}$, we adopt the form in Ref. [63]:

$$
P_{qq}^H = C_F \left[\frac{2x}{(1-x)_+} + \frac{3}{2}\delta(1-x) \right]. \tag{59}
$$

The numerical solution of DGLAP equations is performed by the QCDNUM evolution package [114]. The original code of QCDNUM is modified by us so that the evolution kernels of $\hat{H}_1^{\perp(3)}$ and $h_{1L}^{\perp(1)}$ are included. In Fig. 2, we plot the $h_{1L}^{\perp(1)}(x, Q^2)$ (multiplied by x) vs x for light quark flavors at the initial scale $Q^2 = 2.4$ GeV^2 as well as the evolved scale $Q^2 = 100$ GeV^2. The left panel and the right panel show the results for the up quark and the down quark, respectively. The plots show that the $h_{1L}^{\perp(1)}(x, Q^2)$ for up quark is larger than one for the down quark in size, and with the opposite

Fig. 2 Left panel: $h_{1L}^{\perp(1)}(x, Q^2)$ (multiplied by x) of the proton longitudinal transversity PDF $h_{1L}^{\perp}$ for up quark at $Q^2 = 2.41$ GeV^2 and $Q^2 = 10$ GeV^2. Right panel: similar to the left panel, but for the down quark
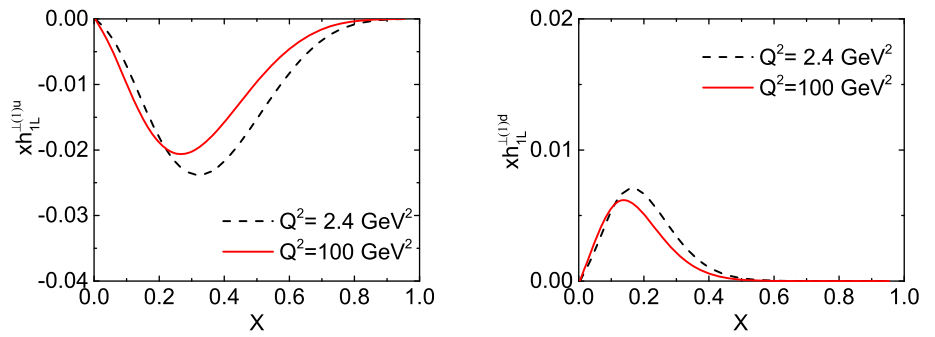
sign for them. Also, the evolution effect from lower scale to higher scale drives the peak of the distribution to the smaller x region.

The $A_{UL}^{\sin 2\phi_h}$ asymmetry pion production was measured at HERMES off the proton target [37,52] and off the deuteron target [38] in the kinematic range

$$1 \,\text{GeV}^2 < Q^2 < 15 \,\text{GeV}^2, \quad W > 2 \,\text{GeV},$$
$$0.023 < x < 0.4, \quad 0.2 < y < 0.85, \quad 0.2 < z < 0.7, \quad (60)$$

while it was also measured for pion production off the proton target by CLAS [39,53] in the kinematic range

$$1 \,\text{GeV}^2 < Q^2 < 5.4 \,\text{GeV}^2, \quad W > 2 \,\text{GeV},$$
$$0.12 < x < 0.48, \quad y < 0.85, \quad 0.4 < z < 0.7, \quad (61)$$

with $W^2 = (P + q)^2 \approx \frac{1-x}{x} Q^2$ being the invariant mass of the virtual photon-nucleon system.

In Figs. 3 and 4, we plot our numerical results of the $\sin 2\phi_h$ azimuthal asymmetry off the longitudinally polarized proton and deuteron target in the SIDIS process at HERMES kinematics [37,38,50–52], based on the TMD factorization formalism described in Eqs. (50), (53) and (54). The solid squares show the experimental data measured by the

HERMES collaboration [37,38,50], with the error bars corresponding to the statistical uncertainty. To make the TMD factorization valid, the integration over the transverse momentum $P_{\pi T}$ is performed in the region of $P_{\pi T} < 0.5$ GeV. In the calculations we apply the EIKV parametrization (dark dashed line) and the BDPRS parametrization (red solid line) for the nonperturbative part. The yellow, green and cyan shaded areas around solid lines show the uncertainty bands due to the uncertainties of the parameters in the BDPRS parametrization, the transversity distribution $h_1(x)$ for calculating $h_{1L}^{\perp(1)}(x)$, and the twist-3 Collins FF $H^{(3)}$, respectively. Since there are only two sources (the transversity distribution $h_1(x)$ for calculating $h_{1L}^{\perp(1)}(x)$ and the twist-3 Collins FF $H^{(3)}$) will contribute to the uncertainties for the dashed lines, the uncertainties of the dashed lines should be smaller than the uncertainties of the solid lines.

As shown in Figs. 3 and 4, in all the cases the $\sin 2\phi_h$ azimuthal asymmetries in the SIDIS process is around 2% at most. The estimated $\sin 2\phi_h$ azimuthal asymmetry for π^+ is negative, while those for π^- and π^0 are positive. The size of the asymmetry for π^- is larger than that for π^+ and π^0. In addition, our estimates also show that the size of the asymmetries increase with increasing x. In the case of the proton target, the results form the EIKV parametrization are close to those from the BDPRS parametrization; while in the
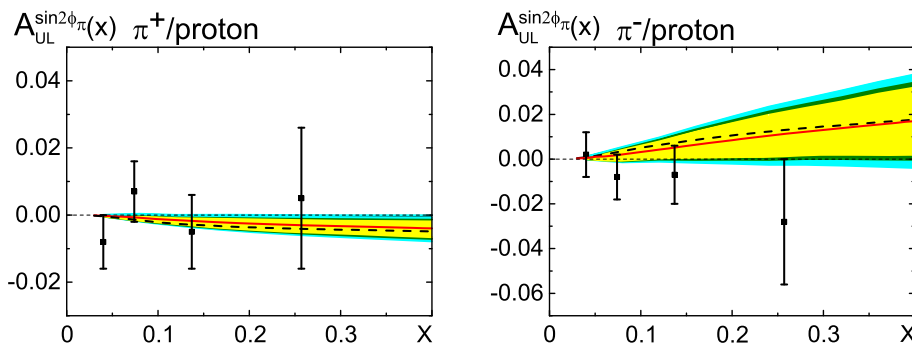

Fig. 3 The $A_{UL}^{\sin 2\phi_h}$ asymmetry for the π^+ (left) and π^- (right) productions off the proton target as function of x at HERMES. The solid lines correspond to the results from the BDPRS parametrization [64] on the nonperturbative form factor, while the dashed lines correspond to the results calculated from the EIKV parametrization [62] on the nonper-

turbative form factor. The yellow, green and cyan shaded areas around solid lines show the uncertainty bands determined by the uncertainties of the parameters in the BDPRS parametrization, the transversity distribution $h_1(x)$ for $h_{1L}^{\perp(1)}(x)$, and twist-3 Collins FF $H^{(3)}$ respectively. The solid squares represent the HERMES data [37,50] for comparison
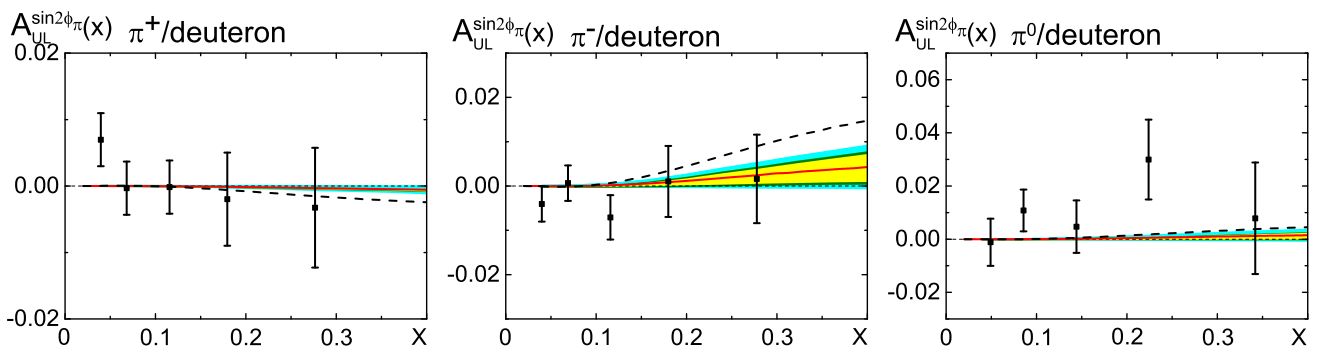
Fig. 4 Similar to Fig. 3, but for π^+ (left), π^- (central) and π^0 (right) productions off the deuteron target. Data from Refs. [38]

Fig. 5 Similar to Fig. 3, but for $A_{UL}^{\sin 2\phi_h}$ as function of x and $P_{\pi T}$ at CLAS kinematics. The upper panels of show the x dependent asymmetries for π^+ (left panel) and π^- (right panel) production, respectively; and the lower panels depict the $x-$ dependent (left panel) and $P_{\pi T}-$ dependent (right panel) asymmetries for π^0 production. The solid squares represent the CLAS data [39,53] for comparison. In each figure we zoom in the plots to show the tendency better
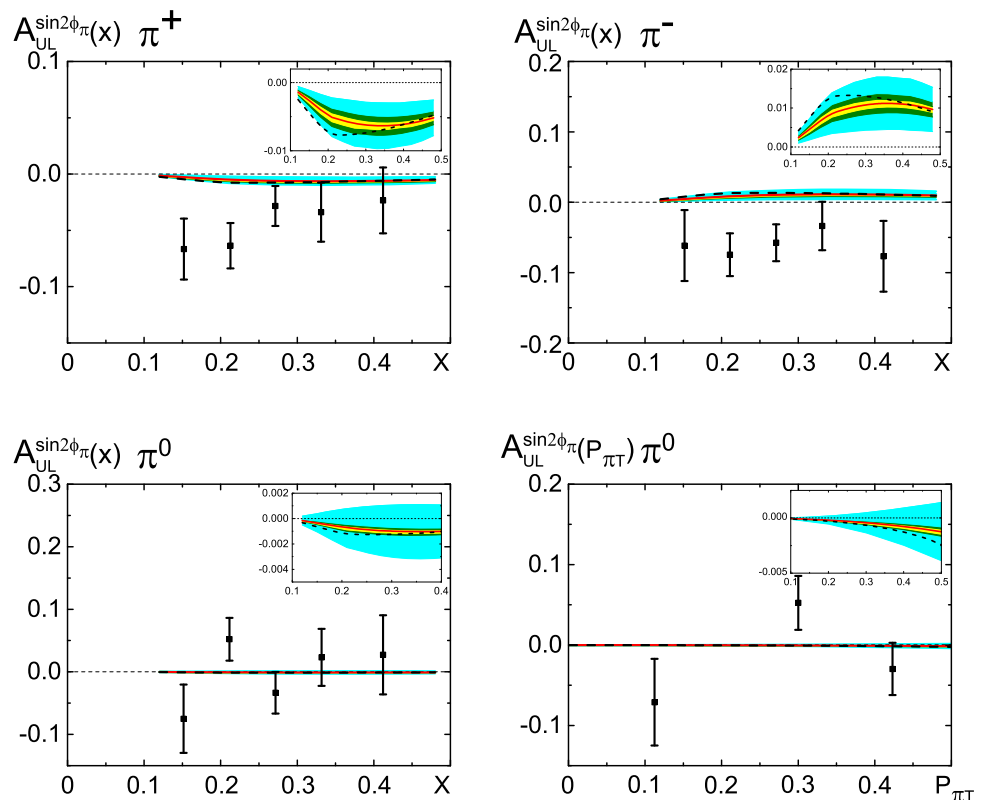
case of the deuteron target, there is quantitative difference between the two parametrization, namely, the results from the EIKV parametrization is two times larger than that from the BDPRS parametrization. From the comparison with the HERMES data, we find that our results are consistent with the HERMES data [37,38,50–52] within the error band, except the π^- production off proton target. In the latter case the computed asymmetry does not agree with the HERMES data, particularly, our calculation and the data has the opposite sign. The possible reason for this inconsistency may be due to the large uncertainties which have not been included in the present calculation. At the end of this section, we will address the source of these uncertainties. A nonzero $\sin 2\phi_h$ azimuthal asymmetries for $\pi^\pm$ are estimated, indicating that

spin-orbit correlation of transversely polarized quarks in the longitudinally polarized nucleon may be significant.

In Fig. 5, we plot our numerical results for the $\sin 2\phi_h$ azimuthal asymmetry off the proton target, but at the CLAS kinematics [39,53]. The upper panels of Fig. 5 show the x-dependent asymmetries of π^+ (left) and π^- (right) production; and the lower panels depict the x-dependent (left) and $P_{\pi T}$-dependent (right) asymmetries of π^0 production. In each figure we zoom in the plots to show the tendency better. Although the uncertainty at CLAS is relatively large, the data indicate that the asymmetries of both π^+ and π^- at CLAS tend to be negative. Thus our estimate miss the data of the x-dependent asymmetry for π^- production. A much smaller $\sin 2\phi$ azimuthal asymmetries for π^0 production is predicted

at CLAS as well as at HERMES off deuteron target, in agreement with experimental data. This is because the favored and unfavored Collins functions is summed for π^0 production, which means that they largely cancel for π^0. Again, the yellow, green and cyan shaded areas around solid lines show the uncertainty bands due to the uncertainties of the parameters in the BDPRS parametrization, the transversity distribution $h_1(x)$ for calculating $h_{1L}^{\perp(1)}(x)$, and the twist-3 Collins FF $H^{(3)}$, respectively.

Even though the $A_{UL}^{\sin 2\phi_h}$ asymmetries off longitudinally polarised targets has been studied at HERMES (proton, deuteron) [37,38,52], CLAS (proton) [39,53] kinematics during the last two decades, there is still no consistent understanding of the contribution of each part to the total structure function which may be due to the low statistics or limited kinematic coverage of previous experiments. Therefore, we also estimate the $A_{UL}^{\sin 2\phi_h}$ asymmetries on proton target for

pion production at the kinematical configuration of CLAS12 experiment [54]

$$1\,\text{GeV}^2 < Q^2 < 7\,\text{GeV}^2, \quad W > 2\,\text{GeV},$$
$$0.13 < x < 0.52, \, y < 0.75, \quad 0.18 < z < 0.7. \tag{62}$$

The estimated asymmetry of π^+ (upper panel), π^- (central panel) and π^0 (lower panel) productions vs x, $P_{\pi T}$ and z are plotted in Fig. 6 respectively. From Fig. 6, we can conclude that the size of the $\sin 2\phi_h$ azimuthal asymmetries at CLAS12 is larger than that at CLAS. Thus, it has a greater opportunity to measure the $\sin 2\phi_h$ asymmetry at CLAS12. Another observation is that the $P_{\pi T}$-dependent asymmetries from the EIKV parametrization and the BDPRS parametrization are somewhat different. These need to be further tested by the future CLAS12 data on the proton target.
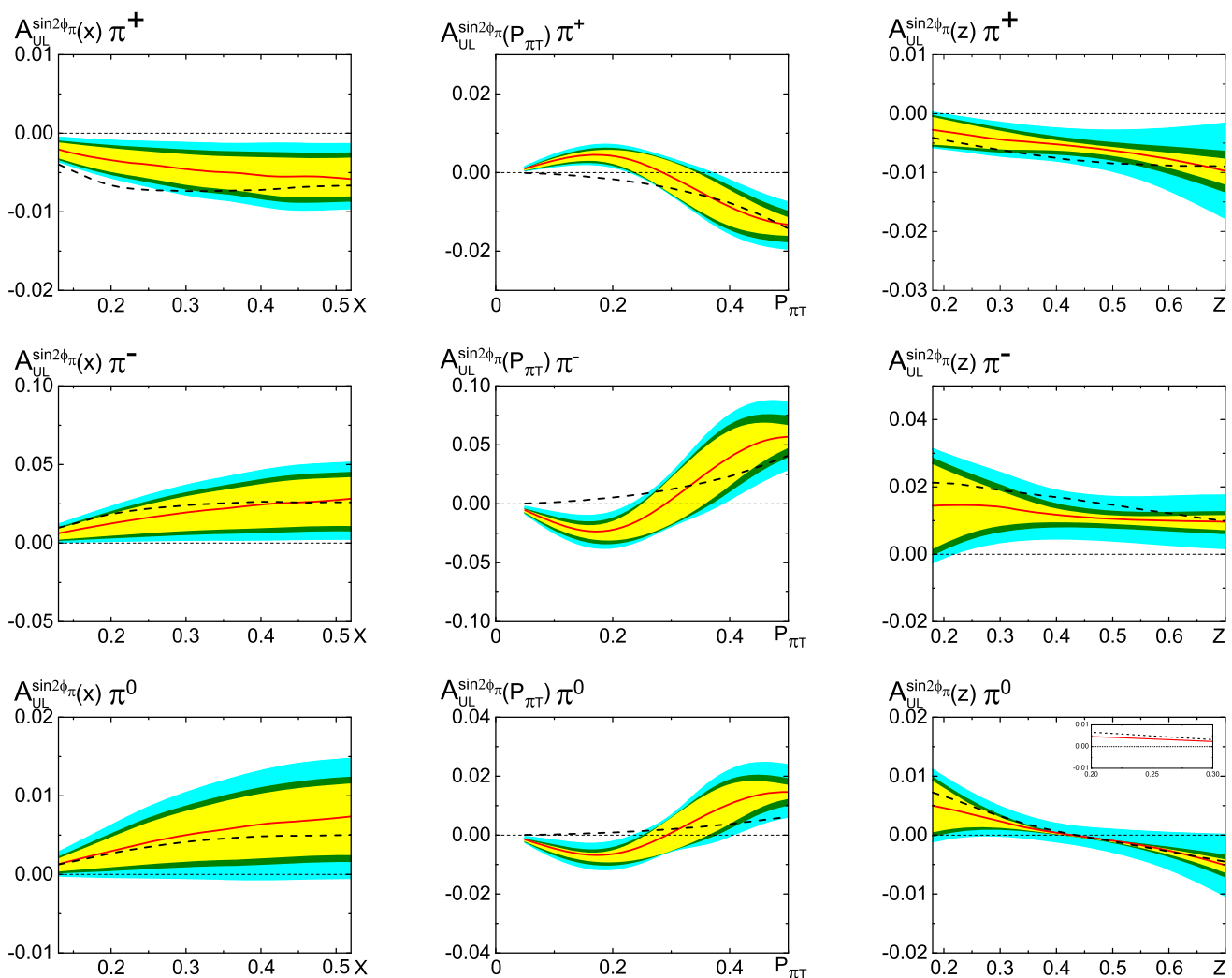

Fig. 6 The $A_{UL}^{\sin 2\phi_h}$ asymmetry as functions of x, $P_{\pi T}$ and z for π^+ (upper panel), π^- (centre panel) and π^0 (lower panel) productions at CLAS12 kinematics

Finally, we would like to comment on the uncertainty from the theoretical aspects. First, one should be cautious on the validation of the TMD factorization in the kinematical region of HERMES and CLAS where Q^2 is not so large. In our calculation we consider the region $P_T < 0.5$ GeV. This should be tested by more precise data in the future. Secondly, as the information on $h_{1L}^\perp$ is still limited, we have to use the WW-approximation to obtain the result of $h_{1L}^\perp$ via the basis function $h_1(x)$, thus the contribution beyond the WW-approximation may also contribute and has not considered in our calculation. Although the data and lattice calculation shows that the WW-approximation works well for the structure function g_2 (or $g_T(x)$), recent study [111] shows that the breaking of the WW-relation can be as large as 15%-40% the size of g_2. This means that in the case of $h_{1L}^\perp$ the higher-twist contribution may be also non-negligible, and the corresponding uncertainty can be 40% of the central value of the asymmetry as a rough estimate. Thirdly, the homogeneous terms of the evolution kernel are applied for $\hat{H}^{(3)}$ and $h_{1L}^{\perp(1)}$. The inhomogeneous terms of the evolution kernel are very complicated, thus they are neglected in the calculation in order to simplify the calculation. This is of course an approximation to the real situation. Fourthly, in the calculation we adopt the NLL result for the perturbative Sudakov form factor. Higher-order QCD corrections can contribute and affect the accuracy of our calculation. If all the uncertainties from the above were taken into account in the calculation properly, the uncertainty bands in Figs. 3, 4, 5, 6 should be much substantial. Further studies are need to clarify these points.

5 Conclusion

In this work, we applied the TMD factorization formalism to study the $\sin 2\phi_h$ asymmetry in SIDIS process at the kinematical configuration of HERMES, CLAS and CLAS12. The asymmetry provides access to the convolution of the TMD distribution $h_{1L}^\perp$, which describes transversely polarized quarks in the longitudinally polarized nucleon, and the Collins function of the pion. We took into account the TMD evolution effects for these TMDs, and we adopted two approaches for the TMD evolution for comparison. One is the EIKV approach, the other is the BDPRS approach. Their main difference is the treatment on the nonperturbative part of evolution, while the perturbative part in the two approaches are the same and was kept at NLL accuracy in this work. As the nonperturbative part associated with $h_{1L}^\perp$ is still unknown, we assumed that it has the same form as that of the unpolarized distribution. The hard coefficients associated with the corresponding collinear functions in the TMD evolution formalism are kept at the leading-order accuracy. We also adopted the WW-type approximations for the longitudinal transversity $h_{1L}^{\perp(1)}(x, \mu)$ of the nucleon and applied

the parametrization for the twist-3 fragmentation function $H_1^{\perp(3)}(z, z, \mu)$ to estimate the asymmetries.

The numerical calculations showed that our results generally agree with the data from HERMES and CLAS within the uncertainty bands, except for x-dependent asymmetry of π^- production off the proton target, for which the sign of the asymmetry is inconsistent. It is also found that the size of the asymmetry off the deuteron target at HERMES is sensitive to the choice of the parametrization for the nonperturbative part of evolution. Similarly, the shape of $P_{\pi T}$−dependent asymmetries from the two parameterizations at CLAS12 are somewhat different. Future precision measurement on the asymmetry may distinguish different parametrization on S_{NP}. We also discussed the uncertainties from the theoretical aspects. For the WW-approximation for $h_{1L}^\perp$, higher-twist part may contribute to the uncertainty band as large as 40% of the central value at most following the WW-breaking effect from the analysis on the structure function g_2. Also, the inhomogeneous terms in the evolution kernel of $h_{1L}^{\perp(1)}$ has not been considered in the calculation which may bring further uncertainty to the result, particular in the small x region, where the effect of these terms can be significant as suggested by the model study on the evolution of $T_{q,F}(x, x)$. Finally, in the calculation we adopted the NLL result for the perturbative Sudakov form factor. Higher-order QCD corrections can contribute and affect the accuracy of our calculation. Further studies are needed on the $\sin 2\phi_h$ asymmetry for a deeper understanding of nucleon structure in three-dimensional space and the validity of WW-type approximation.

Data Availability Statement This manuscript has no associated data or the data will not be deposited. [Authors' comment All the relevant data are already contained in this published article.]

References

1. D.W. Sivers, Phys. Rev. D **41**, 83 (1990)
2. D.W. Sivers, Phys. Rev. D **43**, 261 (1991)

3. M. Anselmino, M. Boglione, F. Murgia, Phys. Lett. B **362**, 164–172 (1995). arXiv:hep-ph/9503290

4. M. Anselmino, F. Murgia, Phys. Lett. B **442**, 470–478 (1998). arXiv:hep-ph/9808426

5. S.J. Brodsky, D.S. Hwang, I. Schmidt, Phys. Lett. B **530**, 99–107 (2002). arXiv:hep-ph/0201296

6. S.J. Brodsky, D.S. Hwang, I. Schmidt, Nucl. Phys. B **642**, 344–356 (2002). arXiv:hep-ph/0206259

7. J.C. Collins, Phys. Lett. B **536**, 43–48 (2002). arXiv:hep-ph/0204004

8. Xd. Ji, F. Yuan, Phys. Lett. B **543**, 66–72 (2002). arXiv:hep-ph/0206057

9. A.V. Belitsky, X. Ji, F. Yuan, Nucl. Phys. B **656**, 165–198 (2003). arXiv:hep-ph/0208038

10. D. Boer, P.J. Mulders, F. Pijlman, Nucl. Phys. B **667**, 201–241 (2003). arXiv:hep-ph/0303034

11. X. Ji, J.W. Qiu, W. Vogelsang, F. Yuan, Phys. Rev. Lett. **97**, 082002 (2006). arXiv:hep-ph/0602239

12. X. Ji, Jw. Qiu, W. Vogelsang, F. Yuan, Phys. Rev. D **73**, 094017 (2006). arXiv:hep-ph/0604023

13. X. Ji, J.W. Qiu, W. Vogelsang, F. Yuan, Phys. Lett. B **638**, 178–186 (2006). arXiv:hep-ph/0604128

14. A. Bacchetta, D. Boer, M. Diehl, P.J. Mulders, JHEP **08**, 023 (2008). arXiv:0803.0227 [hep-ph]

15. P.J. Mulders, R.D. Tangerman, Nucl. Phys. B **461**, 197 (1996) [Erratum: Nucl. Phys. B **484**, 538 (1997)]. arXiv:hep-ph/9510301

16. D. Boer, P.J. Mulders, Phys. Rev. D **57**, 5780–5786 (1998). arXiv:hep-ph/9711485

17. A. Bacchetta, M. Diehl, K. Goeke, A. Metz, P.J. Mulders, M. Schlegel, JHEP **02**, 093 (2007). arXiv:hep-ph/0611265

18. A. Airapetian et al., HERMES. Phys. Rev. Lett. **94**, 012002 (2005). arXiv:hep-ex/0408013

19. A. Airapetian et al., HERMES. Phys. Rev. Lett. **103**, 152002 (2009). arXiv:0906.3918 [hep-ex]

20. A. Airapetian et al., HERMES. Phys. Lett. B **693**, 11–16 (2010). arXiv:1006.4221 [hep-ex]

21. V.Y. Alexakhin et al., COMPASS. Phys. Rev. Lett. **94**, 202002 (2005). arXiv:hep-ex/0503002 [hep-ex]

22. E.S. Ageev et al., COMPASS. Nucl. Phys. B **765**, 31–70 (2007). arXiv:hep-ex/0610068

23. M.G. Alekseev et al., COMPASS. Phys. Lett. B **692**, 240–246 (2010). arXiv:1005.5609 [hep-ex]

24. H. Mkrtchyan, P.E. Bosted, G.S. Adams, A. Ahmidouch, T. Angelescu, J. Arrington, R. Asaturyan, O.K. Baker, N. Benmouna, C. Bertoncini et al., Phys. Lett. B **665**, 20–25 (2008). arXiv:0709.3020 [hep-ph]

25. M. Osipenko et al., CLAS. Phys. Rev. D **80**, 032004 (2009). arXiv:0809.1153 [hep-ex]

26. M. Arneodo et al., European Muon. Z. Phys. C **34**, 277 (1987)

27. J. Breitweg et al., ZEUS. Phys. Lett. B **481**, 199–212 (2000). arXiv:hep-ex/0003017

28. W. Kafer [COMPASS], arXiv:0808.0114 [hep-ex]

29. A. Bressan [COMPASS], arXiv:0907.5511 [hep-ex]

30. S. Falciano et al., NA10. Z. Phys. C **31**, 513 (1986)

31. M. Guanziroli et al., NA10. Z. Phys. C **37**, 545 (1988)

32. L.Y. Zhu et al., NuSea. Phys. Rev. Lett. **100**, 062301 (2008). arXiv:0710.2344 [hep-ex]

33. L.Y. Zhu et al., NuSea. Phys. Rev. Lett. **102**, 182001 (2009). arXiv:0811.4589 [nucl-ex]

34. A. Kotzinian, Nucl. Phys. B **441**, 234–248 (1995). arXiv:hep-ph/9412283 [hep-ph]

35. A.M. Kotzinian, P.J. Mulders, Phys. Lett. B **406**, 373 (1997). arXiv:hep-ph/9701330

36. J.C. Collins, Nucl. Phys. B **396**, 161–182 (1993). arXiv:hep-ph/9208213

37. A. Airapetian et al., HERMES Collaboration. Phys. Rev. Lett. **84**, 4047 (2000). arXiv:hep-ex/9910062

38. A. Airapetian et al., HERMES Collaboration. Phys. Lett. B **562**, 182 (2003). arXiv:hep-ex/0212039

39. H. Avakian et al., CLAS Collaboration. Phys. Rev. Lett. **105**, 262002 (2010). arXiv:1003.4549 [hep-ex]

40. Z. Lu, B.Q. Ma, J. She, Phys. Rev. D **84**, 034010 (2011). arXiv:1104.5410 [hep-ph]

41. J. Zhu, B.Q. Ma, Phys. Lett. B **696**, 246–251 (2011). arXiv:1104.4564 [hep-ph]

42. S. Boffi, A.V. Efremov, B. Pasquini, P. Schweitzer, Phys. Rev. D **79**, 094012 (2009). arXiv:0903.1271 [hep-ph]

43. B.Q. Ma, I. Schmidt, J.J. Yang, Phys. Rev. D **63**, 037501 (2001). arXiv:hep-ph/0009297

44. B.Q. Ma, I. Schmidt, J.J. Yang, Phys. Rev. D **65**, 034010 (2002). arXiv:hep-ph/0110324

45. J.C. Collins, D.E. Soper, Nucl. Phys. B **193**, 381 (1981) [Erratum: Nucl. Phys. B **213**, 545 (1983)]

46. J.C. Collins, D.E. Soper, G.F. Sterman, Nucl. Phys. B **250**, 199 (1985)

47. X.D. Ji, J.P. Ma, F. Yuan, Phys. Rev. D **71**, 034005 (2005). arXiv:hep-ph/0404183

48. Xd. Ji, J.P. Ma, F. Yuan, Phys. Lett. B **597**, 299 (2004). arXiv:hep-ph/0405085

49. J. Collins, Camb. Monogr. Part. Phys. Nucl. Phys. Cosmol. **32**, 1 (2011)

50. H. Avakian [HERMES Collaboration], Nucl. Phys. Proc. Suppl. **79**, 523 (1999)

51. H. Avakian, A.V. Efremov, K. Goeke, A. Metz, P. Schweitzer, T. Teckentrup, Phys. Rev. D **77**, 014023 (2008). arXiv:0709.3253 [hep-ph]

52. A. Airapetian et al., HERMES Collaboration. Phys. Rev. D **64**, 097101 (2001). arXiv:hep-ex/0104005

53. S. Jawalkar et al., CLAS Collaboration. Phys. Lett. B **782**, 662 (2018). arXiv:1709.10054 [nucl-ex]

54. S. Diehl et al. [CLAS], Phys. Rev. Lett. **128**(6), 062005 (2022). arXiv:2101.03544 [hep-ex]

55. D. Boer, Nucl. Phys. B **806**, 23 (2009). arXiv:0804.2408 [hep-ph]

56. S. Arnold, A. Metz, M. Schlegel, Phys. Rev. D **79**, 034005 (2009). arXiv:0809.2262 [hep-ph]

57. S.M. Aybat, T.C. Rogers, Phys. Rev. D **83**, 114042 (2011). arXiv:1101.5057 [hep-ph]

58. J.C. Collins, T.C. Rogers, Phys. Rev. D **87**, 034018 (2013). arXiv:1210.2100 [hep-ph]

59. M.G. Echevarria, A. Idilbi, A. Schäfer, I. Scimemi, Eur. Phys. J. C **73**, 2636 (2013). arXiv:1208.1281 [hep-ph]

60. M.G. Echevarria, A. Idilbi, I. Scimemi, Phys. Lett. B **726**, 795 (2013). arXiv:1211.1947 [hep-ph]

61. D. Pitonyak, M. Schlegel, A. Metz, Phys. Rev. D **89**, 054032 (2014). arXiv:1310.6240 [hep-ph]

62. M.G. Echevarria, A. Idilbi, Z.B. Kang, I. Vitev, Phys. Rev. D **89**, 074013 (2014). arXiv:1401.5078 [hep-ph]

63. Z. B. Kang, A. Prokudin, P. Sun, F. Yuan, Phys. Rev. D **93**(1), 014009 (2016). arXiv:1505.05589 [hep-ph]

64. A. Bacchetta, F. Delcarro, C. Pisano, M. Radici, A. Signori, JHEP **1706**, 081 (2017) [Erratum: JHEP **1906**, 051 (2019)]. arXiv:1703.10157 [hep-ph]

65. X. Wang, Z. Lu, I. Schmidt, JHEP **1708**, 137 (2017). arXiv:1707.05207 [hep-ph]

66. X. Wang, Z. Lu, Phys. Rev. D **97**(5), 054005 (2018). https://doi.org/10.1103/PhysRevD.97.054005. arXiv:1801.00660 [hep-ph]

67. H. Li, X. Wang, Z. Lu, Phys. Rev. D **101**, 054013 (2020). arXiv:1907.07095 [hep-ph]

68. A. Idilbi, Xd. Ji, J.P. Ma, F. Yuan, Phys. Rev. D **70**, 074021 (2004). arXiv:hep-ph/0406302

69. J.C. Collins, F. Hautmann, Phys. Lett. B **472**, 129 (2000). arXiv:hep-ph/9908467
70. C.T.H. Davies, B.R. Webber, W.J. Stirling, Nucl. Phys. B **256**, 413 (1985)
71. R.K. Ellis, D.A. Ross, S. Veseli, Nucl. Phys. B **503**, 309 (1997). arXiv:hep-ph/9704239
72. F. Landry, R. Brock, P.M. Nadolsky, C.P. Yuan, Phys. Rev. D **67**, 073016 (2003). arXiv:hep-ph/0212159
73. A.V. Konychev, P.M. Nadolsky, Phys. Lett. B **633**, 710 (2006). arXiv:hep-ph/0506225
74. S.M. Aybat, J.C. Collins, J.W. Qiu, T.C. Rogers, Phys. Rev. D **85**, 034043 (2012). arXiv:1110.6428 [hep-ph]
75. Z.B. Kang, B.W. Xiao, F. Yuan, Phys. Rev. Lett. **107**, 152002 (2011). arXiv:1106.0266 [hep-ph]
76. P. Sun, J. Isaacson, C.P. Yuan, F. Yuan, Int. J. Mod. Phys. A **33**(11), 1841006 (2018)
77. M.G. Echevarria, A. Idilbi, I. Scimemi, Phys. Rev. D **90**, 014003 (2014). arXiv:1402.0869 [hep-ph]
78. J. Collins, T. Rogers, Phys. Rev. D **91**, 074020 (2015). arXiv:1412.3820 [hep-ph]
79. P.M. Nadolsky, D.R. Stump, C.P. Yuan, Phys. Rev. D **61**, 014003 (2000) [Erratum: Phys. Rev. D **64**, 059903 (2001)]. arXiv:hep-ph/9906280
80. C.A. Aidala, B. Field, L.P. Gamberg, T.C. Rogers, Phys. Rev. D **89**, 094002 (2014). arXiv:1401.2654 [hep-ph]
81. J. Collins, L. Gamberg, A. Prokudin, T.C. Rogers, N. Sato, B. Wang, Phys. Rev. D **94**, 034014 (2016). arXiv:1605.00671 [hep-ph]
82. J.W. Qiu, X.F. Zhang, Phys. Rev. Lett. **86**, 2724 (2001). arXiv:hep-ph/0012058
83. J.W. Qiu, X.F. Zhang, Phys. Rev. D **63**, 114011 (2001)
84. M. Anselmino, M. Boglione, S. Melis, Phys. Rev. D **86**, 014028 (2012)
85. M. Anselmino et al., Phys. Rev. D **71**, 074006 (2005). arXiv:hep-ph/0501196
86. J.C. Collins, A.V. Efremov, K. Goeke, S. Menzel, A. Metz, P. Schweitzer, Phys. Rev. D **73**, 014021 (2006). arXiv:hep-ph/0509076
87. P. Schweitzer, T. Teckentrup, A. Metz, Phys. Rev. D **81**, 094019 (2010). arXiv:1003.2190 [hep-ph]
88. A. Prokudin, P. Sun, F. Yuan, Phys. Lett. B **750**, 533 (2015). arXiv:1505.05588 [hep-ph]
89. J. Zhou, F. Yuan, Z.T. Liang, Phys. Rev. D **81**, 054008 (2010). https://doi.org/10.1103/PhysRevD.81.054008 arXiv:0909.2238 [hep-ph]
90. D. Boer, L. Gamberg, B. Musch, A. Prokudin, JHEP **10**, 021 (2011). arXiv:1107.5294 [hep-ph]
91. D. Boer et al., arXiv:1108.1713 [nucl-th]
92. B. Parsamyan, PoS DIS **2017**, 259 (2018). arXiv:1801.01488 [hep-ex]
93. B. Parsamyan, PoS QCDEV **2017**, 042 (2018)
94. C. Adolph et al. [COMPASS Collaboration], Eur. Phys. J. C **78**(11), 952 (2018) [Erratum: Eur. Phys. J. C **80**(4), 298 (2020)]. arXiv:1609.06062 [hep-ex]
95. M.G. Alekseev et al. [COMPASS Collaboration], Eur. Phys. J. C **70**, 39 (2010). arXiv:1007.1562 [hep-ex]
96. H.L. Lai, M. Guzzi, J. Huston, Z. Li, P.M. Nadolsky, J. Pumplin, C.-P. Yuan, Phys. Rev. D **82**, 074024 (2010). arXiv:1007.2241 [hep-ph]
97. D. de Florian, R. Sassot, M. Stratmann, Phys. Rev. D **75**, 114010 (2007). arXiv:hep-ph/0703242
98. S. Wandzura, F. Wilczek, Phys. Lett. B **72**, 195–198 (1977)
99. R.L. Jaffe, X.D. Ji, Nucl. Phys. B **375**, 527–560 (1992)
100. K. Abe et al., E143. Phys. Rev. D **58**, 112003 (1998). arXiv:hep-ph/9802357
101. P.L. Anthony et al., E155. Phys. Lett. B **553**, 18–24 (2003). arXiv:hep-ex/0204028
102. A. Airapetian et al., HERMES. Eur. Phys. J. C **72**, 1921 (2012). arXiv:1112.5584 [hep-ex]
103. A. Kotzinian, B. Parsamyan, A. Prokudin, Phys. Rev. D **73**, 114017 (2006). arXiv:hep-ph/0603194
104. A. Metz, P. Schweitzer, T. Teckentrup, Phys. Lett. B **680**, 141 (2009). arXiv:0810.5212 [hep-ph]
105. T. Teckentrup, A. Metz, P. Schweitzer, Mod. Phys. Lett. A **24**, 2950 (2009). arXiv:0910.2567 [hep-ph]
106. S. Bastami et al., JHEP **1906**, 007 (2019). arXiv:1807.10606 [hep-ph]
107. M. Gockeler, R. Horsley, W. Kurzinger, H. Oelrich, D. Pleiter, P.E.L. Rakow, A. Schafer, G. Schierholz, Phys. Rev. D **63**, 074506 (2001). arXiv:hep-lat/0011091
108. M. Gockeler, R. Horsley, D. Pleiter, P.E.L. Rakow, A. Schafer, G. Schierholz, H. Stuben, J.M. Zanotti, Phys. Rev. D **72**, 054507 (2005). arXiv:hep-lat/0506017
109. J. Balla, M.V. Polyakov, C. Weiss, Nucl. Phys. B **510**, 327–364 (1998). arXiv:hep-ph/9707515 [hep-ph]
110. B. Dressler, M.V. Polyakov, Phys. Rev. D **61**, 097501 (2000). arXiv:hep-ph/9912376
111. A. Accardi, A. Bacchetta, W. Melnitchouk, M. Schlegel, JHEP **11**, 093 (2009). arXiv:0907.2942 [hep-ph]
112. J. Zhou, F. Yuan, Z.T. Liang, Phys. Rev. D **79**, 114022 (2009). arXiv:0812.4484 [hep-ph]
113. Z.B. Kang, J.W. Qiu, Phys. Rev. D **79**, 016003 (2009). arXiv:0811.3101 [hep-ph]
114. M. Botje, Comput. Phys. Commun. **182**, 490–532 (2011). arXiv:1005.1481 [hep-ph]